

Generating attosecond pulses with controllable polarization from cyclic H_3^{2+} molecules by bichromatic circular fields

Si-Qi Zhang(张思琪), Bing Zhang(张冰), Bo Yan(闫博), Xiang-Qian Jiang(姜向前) and Xiu-Dong Sun(孙秀冬)

Citation: Chin. Phys. B, 2024, 33 (**2**): 023301. DOI: 10.1088/1674-1056/ad062b
Journal homepage: http://cpb.iphy.ac.cn; http://iopscience.iop.org/cpb

What follows is a list of articles you may be interested in

Elliptically polarized high-order harmonic generation in nitrogen molecules with cross-linearly polarized two-color laser fields

Chunyang Zhai(翟春洋), Yinmeng Wu(吴银梦), Lingling Qin(秦玲玲), Xiang Li(李翔), Luke Shi(史璐珂), Ke Zhang(张可), Shuaijie Kang(康帅杰), Zhengfa Li(李整法), Yingbin Li(李盈傧), Qingbin Tang(汤清彬), and Benhai Yu(余本海)
Chin. Phys. B, 2023, 32 (**7**): 073301. DOI: 10.1088/1674-1056/acad70

Generation of quasi-chirp-free isolated attosecond pulses from atoms under the action of orthogonal two-color combined pulse of fundamental frequency and higher intensity second harmonic fields

Rui-Xian Yu(蔚瑞贤), Yue Qiao(乔月), Ping Li(李萍), Jun Wang(王俊), Ji-Gen Chen(陈基根), Wei Feng(冯伟), Fu-Ming Guo(郭福明), and Yu-Jun Yang(杨玉军)
Chin. Phys. B, 2023, 32 (**6**): 063302. DOI: 10.1088/1674-1056/acc80a

Enhancement of isolated attosecond pulse generation by using long gas medium

Yueying Liang(梁玥瑛), Xinkui He(贺新奎), Kun Zhao(赵昆), Hao Teng(滕浩), and Zhiyi Wei(魏志义)
Chin. Phys. B, 2022, 31 (**4**): 043302. DOI: 10.1088/1674-1056/ac29a8

Decoding the electron dynamics in high-order harmonic generation from asymmetric molecular ions in elliptically polarized laser fields

Cai-Ping Zhang(张彩萍) and Xiang-Yang Miao(苗向阳)
Chin. Phys. B, 2022, 31 (**4**): 043301. DOI: 10.1088/1674-1056/ac29b0

Review on non-dipole effects in ionization and harmonic generation of atoms and molecules

Mu-Xue Wang(王慕雪), Si-Ge Chen(陈思格), Hao Liang(梁昊), Liang-You Peng(彭良友)
Chin. Phys. B, 2020, 29 (**1**): 013302. DOI: 10.1088/1674-1056/ab5c10

Generating attosecond pulses with controllable polarization from cyclic H_3^{2+} molecules by bichromatic circular fields

Si-Qi Zhang(张思琪)[1], Bing Zhang(张冰)[1,†], Bo Yan(闫博)[1], Xiang-Qian Jiang(姜向前)[1,‡], and Xiu-Dong Sun(孙秀冬)[1,2]

[1] *School of Physics, Harbin Institute of Technology, Harbin* 150001, *China*
[2] *Collaborative Innovation Center of Extreme Optics, Shanxi University, Taiyuan* 030006, *China*

(Received 14 September 2023; revised manuscript received 11 October 2023; accepted manuscript online 24 October 2023)

We investigate the polarization properties of harmonics from the cyclic H_3^{2+} molecular ions in tailored bichromatic counter-rotating circularly polarized (BCCP) fields by solving the time-dependent Schrödinger equation. The allowed harmonics and their helicities are associated with the symmetry compatibility of the field-target systems, and large intensity difference between adjacent harmonics with opposite helicities appears in a wide spectral range when the BCCP field is at certain rotation angles. We try to explain the intensity difference by using a recombination model based on the quantum-orbit theory and by analyzing the ionization pathways. Moreover, to synthesize attosecond pulse trains with tunable polarization, the intensity difference is manipulated by introducing a seed XUV field, and by changing the relative amplitude ratio as well as the helicity of BCCP fields.

Keywords: high-order harmonic generation, attosecond pulse, multi-center interference

PACS: 33.20.Lg, 42.65.Ky, 42.65.Re **DOI:** 10.1088/1674-1056/ad062b

1. Introduction

High-order harmonic generation (HHG) serves as a table-top source of the extreme ultraviolet (XUV) and soft x-ray light, which is a preferable method to obtain coherent radiation and attosecond pulses (APs).[1–4] Linear APs are restricted in probing chiral-sensitive light-matter interactions,[5,6] so it is desirable to generate APs with tunable polarization. Considerable efforts have been devoted to polarization control of harmonics in elliptically polarized (EP) fields,[7,8] (nearly) orthogonally two-color polarized (OTC) fields,[9–11] and co-rotating bicircular fields.[12] Recently, the bichromatic counter-rotating circularly polarized (BCCP) field with frequencies $(\omega, 2\omega)$ has been proven to be an efficient laser scheme for generating the harmonics with large ellipticity. However, since the adjacent harmonics are counter-rotating,[6,13,14] large intensity difference is required for extending BCCP scheme to generation of highly elliptical attosecond pulses.[13,15–17] For instance, Medišauskas *et al.* pointed out that for p-type states of Ne atoms, large relative intensity of the adjacent harmonics leads to elliptical attosecond pulses both isolated and in a train.[16] In Ref. [17] the authors reported that a right-handed attosecond pulse train (APT) with an ellipticity up to 0.77 and a left-handed APT with an ellipticity of 0.45 can be generated from p-type state of Ne atoms. Until very recently, Dixit *et al.* obtained large relative intensity of the subsequent harmonics from atoms with ground states of s by tuning the relative amplitude ratio of the BCCP field and combining a seed XUV pulse.[18]

It is worth noting that most of the previous works used atoms as targets, but the nonspherical symmetry makes molecules become good candidates for generating (nearly) circularly polarized (CP) harmonics.[19–24] Liu *et al.* found that the allowed harmonics from stereoscopic molecules are sensitive to the molecular orientation which determines the rotational symmetry of the field-target system.[21] Wang *et al.* obtained a right-handed APT with an ellipticity of 0.78 by using the interference between harmonics from degenerate current-carrying orbitals of the CH_3Cl molecule.[22] In addition, researchers investigated the generation of harmonics from cyclic molecules H_n^{q+}, and (nearly) CP harmonics are obtained.[23–25] To the best of our knowledge, the generation of the elliptical APTs using cyclic molecules under a BCCP field, however, has never been realized. In this work, we extend the BCCP scheme to a cyclic molecule target, and investigate polarization of harmonics from H_3^{2+} molecular ions. It is found that, by choosing the rotation angle, large intensity difference appears in pairs of harmonics with alternate helicities in a wide energy region. The intensity difference can be described by a recombination model based on the quantum-orbit (QO) theory, which is associated with the multi-center interference. We also demonstrate the possibility of obtaining APTs with tunable ellipticity and helicity from H_3^{2+}, which can be extended to more complex molecules and various field configurations. For instance, one can utilize BCCP fields with $\omega_1/\omega_2 = \omega/2\omega$ or $\omega_1/\omega_2 = \omega/5\omega$ to irradiate a more stable benzene (C_6H_6)

†Corresponding author. E-mail: zhangbing@hit.edu.cn
‡Corresponding author. E-mail: xqjiang@hit.edu.cn

© 2024 Chinese Physical Society and IOP Publishing Ltd

molecule[26,27] and synthesize elliptical APTs.

2. Theoretical methods

We numerically solve the time-dependent Schrödinger equation (TDSE) with the field-molecule Hamiltonian $H(\boldsymbol{r},t) = \frac{1}{2}\boldsymbol{p}^2 + V_c(\boldsymbol{r}) + \boldsymbol{r}\cdot\boldsymbol{E}(t)$. The BCCP field $\boldsymbol{E}_{\rm bccp}(t)$ and the seed XUV field $\boldsymbol{E}_{\rm xuv}(t)$ are polarized in x–y plane, propagating along the z-axis, which are defined as

$$\begin{aligned}\boldsymbol{E}_{\rm bccp}(t) = f(t)\{&[E_\omega\cos(\omega t) + E_{2\omega}\cos(2\omega t)]\boldsymbol{e}_x \\ &+ \zeta[E_\omega\sin(\omega t) - E_{2\omega}\sin(2\omega t)]\boldsymbol{e}_y\}, \quad (1a)\end{aligned}$$

$$\boldsymbol{E}_{\rm xuv}(t) = E_{\rm xuv} f(t)[\cos(\omega_{\rm xuv}t)\boldsymbol{e}_x + \sin(\omega_{\rm xuv}t)\boldsymbol{e}_y], \quad (1b)$$

$$\boldsymbol{E}_{\rm bccp,xuv}(t) = \boldsymbol{R}(\varphi)[\boldsymbol{E}_{\rm bccp}(t) + \boldsymbol{E}_{\rm xuv}(t)], \quad (1c)$$

where $f(t)$ is a trapezoidal envelope in duration of nine optical cycles ($T_0 = 2\pi/\omega$) and linear ramps of two cycles; E_ω, $E_{2\omega}$ and $E_{\rm xuv}$ are the amplitudes of the fundamental field, the 2ω field and the seed XUV field, respectively; $\zeta = 1$ represents an RL-bicircular field (the fundamental field is right-handed (R) polarized and the 2ω field is left-handed (L) polarized), and $\zeta = -1$ represents an LR-bicircular field. The Lissajous curve of the BCCP field with $E_\omega = E_{2\omega}$ in one optical cycle is shown in Fig. 1(a). Here, φ is the rotation angle of the driving field relative to the molecule illustrated in Fig. 1(b) and $\boldsymbol{R}(\varphi)$ is the rotation matrix.

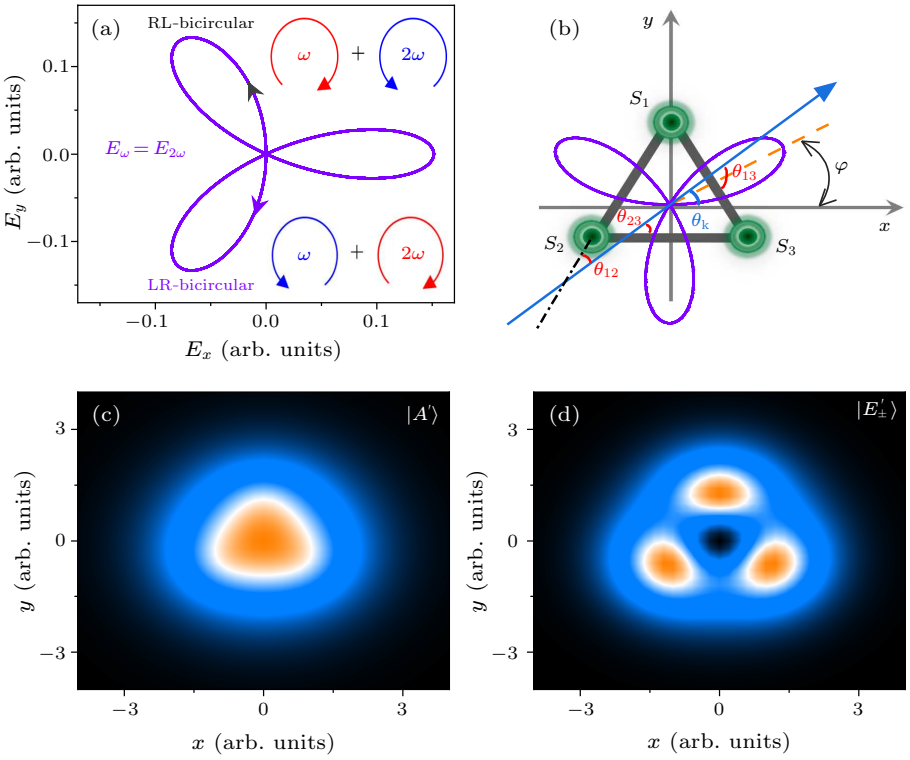


Fig. 1. (a) The Lissajous curve of the BCCP field (ω, 2ω) with amplitudes $E_\omega = E_{2\omega}$. The insets show RL- and LR-bicircular fields obtained by combining the ω and 2ω fields with different helicities. (b) A sketch of cyclic H_3^{2+} molecular ions in the BCCP field at a rotation angle φ. The blue arrow represents the recombination direction of the electron; θ_k is the return angle of the electron relative to the x-axis; θ_{12}, θ_{23} and θ_{13} are angles between internuclear vectors and the momentum of the return electron. [(c), (d)] The electronic density distributions of (c) the ground state $|A'\rangle$ and (d) the degenerate excited states $|E'_\pm\rangle$ of H_3^{2+}.

The molecular ion H_3^{2+} is aligned in the xoy plane and the Coulomb potential is written as

$$V_c(\boldsymbol{r}) = \sum_{i=1}^{n} -\frac{1}{\sqrt{|\boldsymbol{r}-\boldsymbol{R}_i|^2 + \beta}}, \quad (2)$$

where $\boldsymbol{R}_i$ is the fixed position of the i-th atomic center, and the nuclear coordinates (N_{ix}, N_{iy}) are $[N_{1x} = 0,\ N_{1y} = (2/3)R\cos(\vartheta/2)]$, $[N_{2x} = -R\sin(\vartheta/2),\ N_{2y} = -(1/3)R\cos(\vartheta/2)]$, $[N_{3x} = R\sin(\vartheta/2),\ N_{3y} = -(1/3)R\cos(\vartheta/2)]$ with the angle $\vartheta = 60^\circ$ between two molecular bonds, where $R = 2$ a.u. is the distance between two protons. The soft-core parameter is $\beta = 0.35$. The three lowest electronic states of H_3^{2+} are the ground state $|A'\rangle$ and the degenerate excited states $|E'_\pm\rangle$ with ionization potentials $I_p(A') = 1.8$ a.u. and $I_p(E'_\pm) = 1.2$ a.u. The $|E'_\pm\rangle$ states can be defined as $|E'_\pm\rangle = (|E^{(1)}\rangle \pm i|E^{(2)}\rangle)/\sqrt{2}$ with electron angular momentum $m = \pm 1$. Here, $|E^{(1)}\rangle$ and $|E^{(2)}\rangle$ are two orthogonal degenerate real states, which can be obtained by the imaginary-time evolution method.[25,28] Similar to the atomic configuration, an electron in $|E'_+\rangle$ orbital ($m = +1$) circulates in the same sense as the right-handed circularly polarized fields, while the $|E'_-\rangle$ orbital ($m = -1$) is counterrotating.[29] The electronic density distributions of these three states are shown in Figs. 1(c) and 1(d), and a sketch of molecule in a BCCP field is presented in Fig. 1(b).

The TDSE is numerically solved by the split-operator

method with the time step $\Delta t = 0.05$ a.u.[30] The computation space is $L_x \times L_y = 204.8 \times 204.8$ a.u. with 1024×1024 grid points. At each time step, a mask function in the form of $\cos^{1/8}$ has been used to avoid the unphysical reflection of the electron wave packet with an absorbing boundary $3L_{x(y)}/8$. Once the dipole acceleration $\boldsymbol{a}(t)$ has been obtained, the $x(y)$ component of the intensity of one harmonic with frequency $\Omega = n\omega$ can be obtained by

$$P_{x(y)}(\Omega) = \left| \int a_{x(y)}(t)\, \mathrm{e}^{-\mathrm{i}\Omega t}\, \mathrm{d}t \right|^2. \tag{3}$$

The ellipticity of the HHG is defined as $\varepsilon_{\mathrm{h}} = (|a_+| - |a_-|)/(|a_+| + |a_-|)$, with $a_\pm = \frac{1}{\sqrt{2}}[a_x(\Omega) \pm \mathrm{i} a_y(\Omega)]$, where $a_x(\Omega)$ and $a_y(\Omega)$ are the x and y components of dipole acceleration in the frequency domain, respectively.[31,32] Then, the right- and left-handed polarized HHG components can be given by $D_\pm = |a_\pm|^2$. The phase difference between the x and y components is $\delta = \phi_x(\Omega) - \phi_y(\Omega)$ with $\phi_{x(y)}(\Omega) = \arg[a_{x(y)}(\Omega)]$.

3. Results and discussions

Due to the symmetry compatibility of the field-target systems,[24,25] the $3n$-order harmonics are forbidden for the three lowest states ($|A'\rangle$ and $|E'_\pm\rangle$) of H_3^{2+}. In the RL-bicircular field case, harmonics with orders $(3n+1)$ are right-handed polarized, and with $(3n-1)$ orders are left-handed polarized. Firstly, H_3^{2+} is initially prepared on the ground state $|A'\rangle$ and is driven by an RL-bicircular field with intensities $I_\omega = I_{2\omega} = 2 \times 10^{14}$ W/cm^2 ($E_\omega = E_{2\omega} = 0.075$ a.u.) and with frequencies $\omega = 0.057$ a.u. ($\lambda = 800$ nm), $2\omega = 0.114$ a.u. ($\lambda_2 = 400$ nm). By scanning the rotation angle, we find that the intensity difference between adjacent harmonics with alternating helicities depends on the rotation angle φ of the driving field and is large in a wide energy region at $\varphi = 30°$. The harmonic spectra $P_{x(y)}(\Omega)$ are presented in Fig. 2(a). The cutoff order is $N_{\mathrm{c}} = 75\omega$, which is in good agreement with the prediction obtained by the recollision model of bicircular fields.[25] Figure 2(c) shows that the ellipticity of most harmonics deviates from perfect circular polarization ($|\varepsilon_{\mathrm{h}}| \leq 1$), and this deviation originates from the imperfect overlap between the x and y components of the harmonics, which could be attributed to the temporal asymmetry caused by the fast variation of fields on the rising and falling edges.[33] The resolved harmonic components with right- and left-hand polarizations are shown in Fig. 2(b) and the intensity difference of the adjacent harmonics oscillates with orders. However, from the insets, one can clearly see that the left-handed harmonics (blue short dot-dashed) are stronger than the right-handed ones (red solid) from 39th to 57th orders. Thus, elliptical APTs with left-handed polarization can be synthesized by using these harmonics, which will be discussed in detail later.

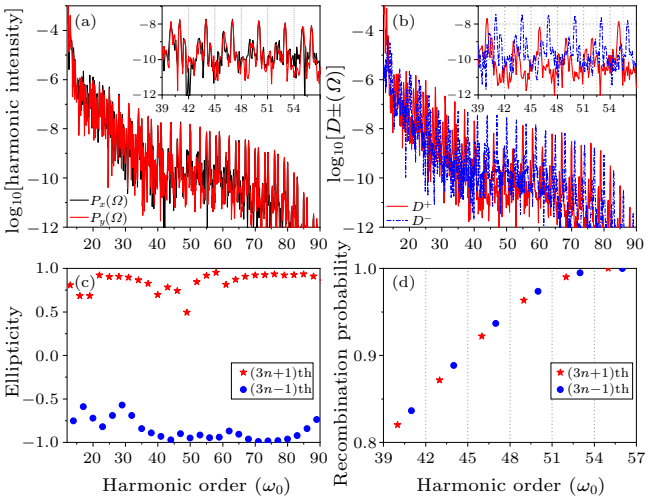


Fig. 2. (a) Harmonic spectra $P_{x(y)}(\Omega)$ from the ground state $|A'\rangle$ of H_3^{2+} in an RL-bicircular field with wavelengths $\lambda = 800$ nm, $\lambda_2 = 400$ nm at a rotation angle $\varphi = 30°$. The intensities of driving field are $I_\omega = I_{2\omega} = 2 \times 10^{14}$ W/cm^2 ($E_\omega = E_{2\omega} = 0.075$ a.u.). (b) The resolved harmonic components with right and left-hand polarization $D_\pm$. (c) Ellipticity of the allowed harmonics. (d) The recombination probability of the harmonics. The detailed harmonic spectra from 39th to 57th orders are shown in the insets.

In the following, we try to interpret the intensity difference between the adjacent harmonics from a view of multicenter interference. In the molecular orbital theory, each orbital of H_3^{2+} is a linear combination of three H atomic 1s orbitals,

$$\psi_{A'} = [\psi_{\mathrm{s}_1} + \psi_{\mathrm{s}_2} + \psi_{\mathrm{s}_3}]/\sqrt{3}, \tag{4a}$$

$$\psi_{E'_-} = [\psi_{\mathrm{s}_1} + \mathrm{e}^{-2\pi\mathrm{i}/3}\psi_{\mathrm{s}_2} + \mathrm{e}^{2\pi\mathrm{i}/3}\psi_{\mathrm{s}_3}]/\sqrt{3}, \tag{4b}$$

$$\psi_{E'_+} = [\psi_{\mathrm{s}_1} + \mathrm{e}^{2\pi\mathrm{i}/3}\psi_{\mathrm{s}_2} + \mathrm{e}^{-2\pi\mathrm{i}/3}\psi_{\mathrm{s}_3}]/\sqrt{3}. \tag{4c}$$

Since interference between two nuclei cannot be changed by the presence of a third nucleus, considering the interference of each pair of nuclei, the recombination matrix elements for the three states are given by[34]

$$\boldsymbol{d}_{\mathrm{rec}}^{A'}(\boldsymbol{k}, \boldsymbol{R}) \propto \cos(\boldsymbol{k}\boldsymbol{R}_{12}/2) + \cos(\boldsymbol{k}\boldsymbol{R}_{23}/2) + \cos(\boldsymbol{k}\boldsymbol{R}_{13}/2), \tag{5a}$$

$$\boldsymbol{d}_{\mathrm{rec}}^{E'_-}(\boldsymbol{k}, \boldsymbol{R}) \propto \cos(\boldsymbol{k}\boldsymbol{R}_{12}/2 - \pi/3) + \cos(\boldsymbol{k}\boldsymbol{R}_{23}/2 - 2\pi/3) + \cos(\boldsymbol{k}\boldsymbol{R}_{13}/2 - \pi/3), \tag{5b}$$

$$\boldsymbol{d}_{\mathrm{rec}}^{E'_+}(\boldsymbol{k}, \boldsymbol{R}) \propto \cos(\boldsymbol{k}\boldsymbol{R}_{12}/2 + \pi/3) + \cos(\boldsymbol{k}\boldsymbol{R}_{23}/2 + 2\pi/3) + \cos(\boldsymbol{k}\boldsymbol{R}_{13}/2 + \pi/3), \tag{5c}$$

where $\boldsymbol{k}$ is the recombination momentum of electrons, $\boldsymbol{R}_{ij} = \boldsymbol{R}_i - \boldsymbol{R}_j$ is the internuclear vector. As illustrated in Fig. 1(b), the angle between $\boldsymbol{k}$ and three internuclear vectors can be expressed as $|\theta_{12}| = |\theta_k - \vartheta|$, $|\theta_{23}| = |\theta_k|$, and $|\theta_{13}| = |\theta_k + \vartheta|$. Then the corresponding recombination probabilities read

$$R_{\mathrm{rec}}^{A'}(R, \theta_k) \propto \cos^2[k(R/2)\cos(\theta_k - \vartheta)] + \cos^2[k(R/2)\cos\theta_k] + \cos^2[k(R/2)\cos(\theta_k + \vartheta)], \tag{6a}$$

$$R_{\mathrm{rec}}^{E'_-}(R, \theta_k) \propto \cos^2[k(R/2)\cos(\theta_k - \vartheta) - \pi/3]$$

$$+\cos^2[k(R/2)\cos\theta_k - 2\pi/3]$$
$$+\cos^2[k(R/2)\cos(\theta_k+\vartheta)-\pi/3], \quad (6b)$$

$$R^{E'_+}_{\rm rec}(R,\theta_k) \propto \cos^2[k(R/2)\cos(\theta_k-\vartheta)+\pi/3]$$
$$+\cos^2[k(R/2)\cos\theta_k + 2\pi/3]$$
$$+\cos^2[k(R/2)\cos(\theta_k+\vartheta)+\pi/3]. \quad (6c)$$

Here, we use the effective momentum $k=\sqrt{2\Omega}$ that considers the Coulomb acceleration, and define θ_k as the return angle of the recombination electrons relative to the x-axis [Fig. 1(b)]. In the QO model, the return angle θ_k can be calculated by using the saddle-point equations

$$\frac{[\boldsymbol{p}(t_1,t_2)+\boldsymbol{A}(t_1)]^2}{2} = I_p, \quad (7a)$$
$$\frac{[\boldsymbol{p}(t_1,t_2)+\boldsymbol{A}(t_2)]^2}{2} = \Omega - I_p. \quad (7b)$$

Here, $\boldsymbol{p}(t_1,t_2)=\frac{-1}{(t_2-t_1)}\int_{t_1}^{t_2}\boldsymbol{A}(t')\mathrm{d}t'$ is the saddle-point momentum with $\boldsymbol{A}(t)=-\int_0^t \boldsymbol{E}(t')\mathrm{d}t'$, t_1 and t_2 are ionization and return times of the electrons. In this case, the return velocity takes the form $\boldsymbol{v}_r(t_2)=\boldsymbol{p}(t_1,t_2)+\boldsymbol{A}(t_2)$, and the return angle has the expression of $\theta_k=\arctan(\mathrm{Re}[v_{y,r}]/\mathrm{Re}[v_{x,r}])$.[35] Figure 2(d) shows the normalized recombination probability of the above-threshold harmonics from $|A'\rangle$ state. The recombination probability of left-handed harmonics (blue disks) is larger than right-handed ones (red stars) from 39th to 57th. Since the photoionization matrix elements are the complex conjugate of the recombination, our analysis can be extended to the ionization process. In a BCCP field (ω, 2ω), the frequency of kth harmonic is $\Omega=p\omega+2q\omega$, where p and q are the number of absorbed photons from ω and 2ω fields, respectively. For s-type state of atoms ($p=q\pm1$), $\Omega^{(3q+1)}=(q+1)\omega+2q\omega$ harmonics corotate with the ω field, and $\Omega^{(3q-1)}=(q-1)\omega+2q\omega$ harmonics corotate with the 2ω field. In the case of $I_\omega=I_{2\omega}$, a pair of odd-even harmonics are of similar intensities, producing an approximately linearly polarized attosecond pulse.[16,36] However, the generation of kth molecular harmonic comes from various $(p;q)$ combinations,[37] and the interplay between $p>q$ and $p<q$ pathways leads to intensity difference between adjacent harmonics, which are promising for synthesizing attosecond pulse with tunable polarization. For the RL-bicircular field discussed above, $p>q$ pathways (the electron absorbs more photons from the ω field) dominate the right-handed polarized $(3n+1)$ harmonics, while $p<q$ pathways dominate the left-handed $(3n-1)$ orders. Therefore, from the recombination probability in Fig. 2(d), we can deduce that the dominance of $p<q$ pathways in $(3n-1)$ harmonics is more obvious than that of $p>q$ pathways in $(3n+1)$ orders, leading to strong left-handed harmonics. Our conclusion here is in good agreement with that Medišauskas obtained from propensity rules for the p state of a model Ne atom.[16]

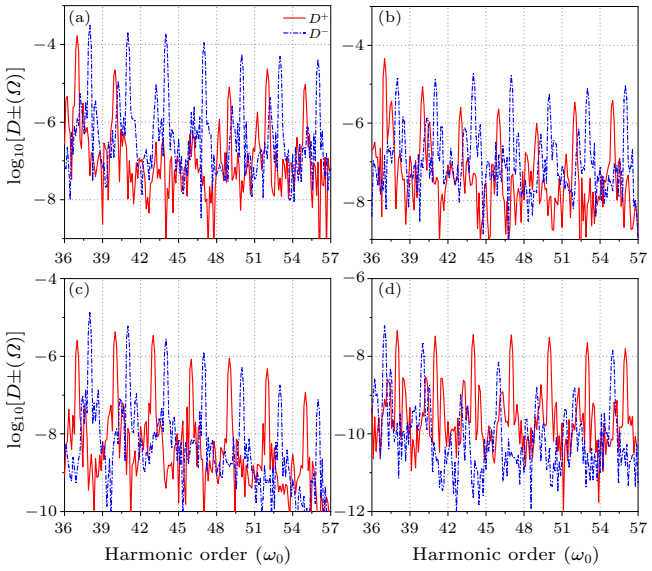


Fig. 3. The resolved harmonic components with right and left-hand polarization $D_\pm$ from $|A'\rangle$ state of the H_3^{2+} driven by an RL-bicircular field, (a) in combination with a left-handed XUV field with frequency $\omega_{\rm xuv}=11\omega$, (b) in combination with a right-handed XUV field with frequency $\omega_{\rm xuv}=10\omega$, (c) for the amplitude of the 2ω field reduced to $2E_{2\omega}=E_\omega=0.075$ a.u. and the right-handed XUV field still on. (d) The LR-bicircular field is used. Other laser parameters are the same as those in Fig. 2

In the following, we try to control the intensity difference between adjacent harmonics by tailoring the BCCP field, so that we could obtain APTs with tunable polarization. We introduce an XUV field co-rotating with the 2ω field to seed harmonic generation. This seed field could enhance the chance of absorbing photons from the 2ω field versus the ω field, and its amplitude and frequency are $E_{\rm xuv}=0.01$ a.u. and $\omega_{\rm xuv}=11\omega$, respectively. The detailed harmonics in Fig. 3(a) show that all harmonics are enhanced by the seed field, and the enhancement of left-handed harmonics is larger than that of the right-handed ones except for 50th and 53rd. As a result, the intensity difference between adjacent harmonics becomes larger and the ellipticity of the generated APTs increases. We mention that the 46th harmonic changes from the right-handed to left-handed polarization. That may be due to the fact that the driving field is not strictly three-fold rotational symmetric due to the presence of the seed field, and the symmetry breaking leads to the helicity reverse of specific harmonic. To obtain APTs with right-handed polarization, we need to make the right-handed harmonics dominant. Then, a right-handed XUV with frequency $\omega_{\rm xuv}=10\omega$ is introduced, but the effect is not obvious. Most of the right-handed harmonics are enhanced slightly more than left-handed ones, but left-handed harmonics still dominate in the spectrum [see Fig. 3(b)]. To further enhance the right-handed harmonics, we reduce the amplitude of the 2ω field to $2E_{2\omega}=E_\omega=0.075$ a.u. to increase the chance of absorbing photons from the ω field. However, the reduction of 2ω field only makes the intensities of the left- and right-handed harmonics comparable to each other [see Fig. 3(c)]. Finally, we have to change the helicity of the driving field and

use an LR-bicircular field. In this case, $(3n\pm1)$ harmonics with reversed helicities are produced and the right-handed harmonics become dominant [see Fig. 3(d)], thus a right-handed polarized APT can be synthesized. From the above discussion, we can conclude that the introduction of an XUV field co-rotating with the stronger left-handed harmonics leads to the enhancement of the intensity difference of left- and right-handed harmonics, yielding left-handed polarized APT with a larger ellipticity. In addition, a right-handed polarized APT can be obtained by changing the helicity of the bicircular field.

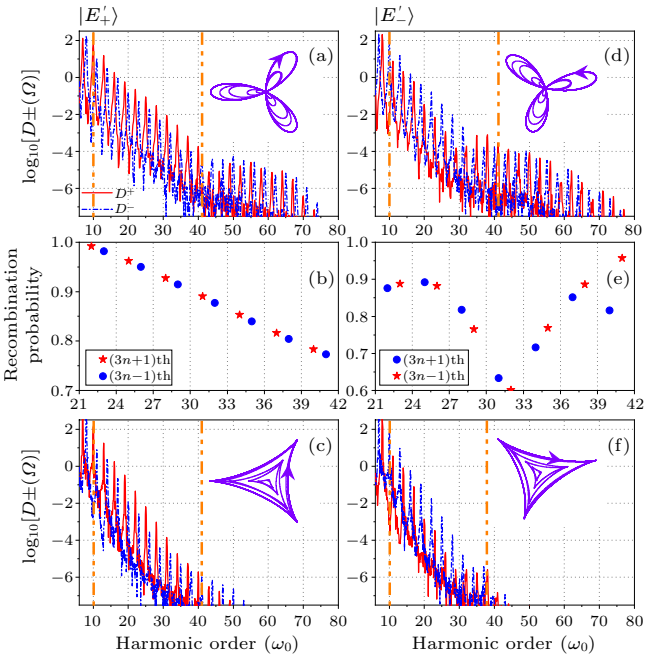


Fig. 4. The resolved harmonic components with right and left-hand polarization $D_\pm$ from the $|E'_+\rangle$ state of the H_3^{2+} in RL-bicircular field at $\varphi = 60^\circ$ with amplitudes (a) $E_\omega = E_{2\omega} = 0.075$ a.u., (c) $2E_{2\omega} = E_\omega = 0.075$ a.u. The resolved harmonic components $D_\pm$ from the $|E'_-\rangle$ state in LR-bicircular field at $\varphi = 15^\circ$ with (d) $E_\omega = E_{2\omega} = 0.075$ a.u., (f) $2E_{2\omega} = E_\omega = 0.075$ a.u. Other laser parameters are the same as those in Fig. 2. The Lissajous curves of the electric fields are shown in the insets. The recombination probability of the harmonics (H21-H42) from (b) $|E'_+\rangle$ and (e) $|E'_-\rangle$ states.

Secondly, H_3^{2+} is initially prepared on $|E'_+\rangle$ state, and we find that large intensity difference is achieved in a broad spectral range for $|E'_+\rangle$ state under RL-bicircular field with $\varphi = 60^\circ$, where the right-handed $(3n+1)$ harmonics are stronger than left-handed $(3n-1)$ orders from 10th to 42nd orders, as shown in Fig. 4(a). The recombination probability in Fig. 4(b) shows the same tendency, so we can deduce that the prominent dominance of $p > q$ pathways in $(3n+1)$ harmonics result in right-handed harmonics stronger than left-handed ones in this energy region. As is expected, when we reduce the amplitude of the 2ω field to $2E_{2\omega} = E_\omega = 0.075$ a.u., the dominance of right-handed harmonics is intensified [see Fig. 4(c)]. Analogously, an LR-bicircular field with $\varphi = 15^\circ$ is used for the $|E'_-\rangle$ state, in which the $(3n+1)$ harmonics are left-handed polarized and $(3n-1)$ harmonics are right-handed polarized, as shown in Fig. 4(d). We can see that left-handed harmonics are stronger than right-handed ones from 10th to 32nd orders, and a reversed result can be observed from 33rd to 42nd orders. The recombination probability of harmonics in Fig. 4(e) reproduces the trend again. When the 2ω field is reduced to $2E_{2\omega} = E_\omega = 0.075$ a.u., the energy region dominated by the left-handed harmonics extends to a range from 10th to 38th orders [Fig. 4(f)].

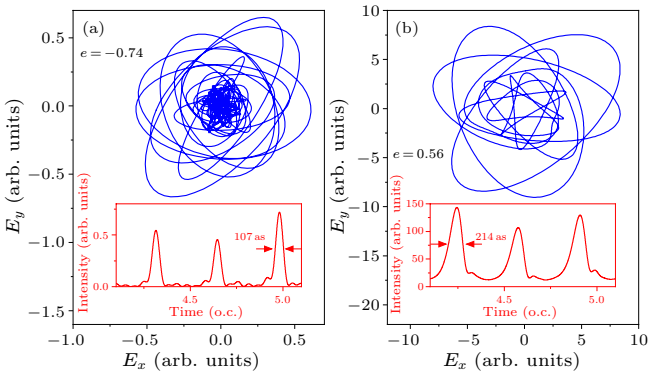


Fig. 5. The electric fields of the APTs synthesized by harmonics (a) from the $|A'\rangle$ state under an RL-bicircular field with amplitudes $E_\omega = E_{2\omega} = 0.075$ a.u. in combination with a left-handed XUV field, (b) from the $|E'_+\rangle$ state under an RL-bicircular field with $2E_{2\omega} = E_\omega = 0.075$ a.u. The insets show temporal profiles of the APTs.

According to the above discussion, we have obtained large intensity difference between adjacent harmonics with alternating helicities in a wide energy region by tailoring the bicircular field. APTs with high ellipticity can be synthesized by using these harmonics, and we present two typical results in Fig. 5. The ellipticity of the APTs can be defined as $e = (|E_+|^2 - |E_-|^2)/(|E_+|^2 + |E_-|^2)$,[17] where E_+ and E_- are calculated by integrating the two counter-rotating components $E_\pm = \mp(E_x + iE_y)/\sqrt{2}$ of the electric field over a temporal window (4.1–5.1 optical cycles). Firstly, by superposing 37th to 56th harmonics from the $|A'\rangle$ state under an RL-bicircular field [Fig. 2(b)], we obtain a left-handed polarized APT with an ellipticity of $e = -0.59$ (not shown here). As mentioned above, using a left-handed XUV as the seed field can improve the intensity difference between adjacent harmonics. Consequently, a left-handed polarized APT with an ellipticity up to $e = -0.74$ is generated [Fig. 5(a)]. From the inset, we can see that there are three attosecond bursts in one optical cycle, and the duration of the most intense burst is 107 as, which is shorter than the one up to 213 as long we obtained from H_2^+ molecules under an OTC field.[38] Figure 5(b) presents electric field of the APT obtained by superposing 10th to 35th harmonics from the $|E'_+\rangle$ state under an RL-bicircular field with $2E_{2\omega} = E_\omega = 0.075$ a.u. [Fig. 4(c)], a right-handed polarized APT with $e = 0.56$ is obtained and the duration of the most intense burst is 214 as. Our simulations show the viability of extending the BCCP scheme to molecule targets, and the control of the harmonic chirality inherently allows one to manipulate the polarization of the generating APTs.

4. Conclusions

In summary, we theoretically study the harmonic radiation from cyclic H_3^{2+} molecular ions under tailored BCCP fields with frequencies $(\omega, 2\omega)$ by numerically solving TDSE. Due to compatible symmetry of the field and molecular orbital, the allowed harmonics with $(3n \pm 1)$ order are counter-rotating to each other. Our simulations show that large intensity difference between adjacent harmonics in a wide energy range can be obtained by choosing the rotation angles of the BCCP field. The intensity difference is interpreted by using a recombination model, and we deduce that the strong recombination corresponds to an intense ionization process related to certain pathways. In other words, harmonics co-rotating with the fundamental field are dominant when the pathways corresponding to electrons absorbing more photons from the fundamental field show prominent dominance, and vice versa. To further control the ellipticity and helicity of the synthesized APTs, we tailor the BCCP fields by introducing XUV pulse, reducing the amplitude of 2ω field, or even changing the helicity of the driving field. Using these methods, a left-handed APT with an ellipticity up to 0.74 and a right-handed APT with an ellipticity of 0.56 are obtained. Our work would provide a reference for manipulating the polarization of the generating APTs in molecular systems.

Acknowledgments

This work was supported by the National Natural Science Foundation of China (Grant No. 91950117) and the Fundamental Research Funds for the Central Universities.

References

[1] Sansone G, Benedetti E, Calegari F, Vozzi C, Avaldi L, Flammini R, Poletto L, Villoresi P, Altucci C, Velotta R, Stagira S, De Silvestri S and Nisoli M 2006 *Science* **314** 443
[2] Paul P M, Toma E S, Breger P, Mullot G, Auge F, Balcou P, Muller H G and Agostini P 2001 *Science* **292** 1689
[3] Wang X W, Wang L, Xiao F, Zhang D W, Lü Z H, Yuan J M and Zhao Z X 2020 *Chin. Phys. Lett.* **37** 023201
[4] Xia C L and Miao X Y 2015 *Chin. Phys. Lett.* **32** 043202
[5] Zhou X, Lock R, Wagner N, Li W, Kapteyn H C and Murnane M M 2009 *Phys. Rev. Lett.* **102** 073902
[6] Huang P C, Hernández-García C, Huang J T, Huang P Y, Lu C H, Rego L, Hickstein D D, Ellis J L, Jaron-Becker A, Becker A, Yang S D, Durfee C G, Plaja L, Kapteyn H C, Murnane M M, Kung A H and Chen M C 2018 *Nat. Photon.* **12** 349
[7] Sun F J, Chen C, Li W Y, Liu X, Li W and Chen Y J 2021 *Phys. Rev. A* **103** 053108
[8] Huo X X, Wang S, Sun L, Xing Y H, Zhang J and Liu X S 2022 *Phys. Rev. A* **106** 023102
[9] Zhai C, Shao R, Lan P, Wang B, Zhang Y, Yuan H, Njoroge S M, He L and Lu P 2020 *Phys. Rev. A* **101** 053407
[10] Zhai C, Wu Y, Qin L, Li X, Shi L, Zhang K, Kang S, Li Z, Li Y, Tang Q and Yu B 2023 *Chin. Phys. B* **32** 073301
[11] Habibović D, Becker W and Milošević D B 2022 *Phys. Rev. A* **106** 023119
[12] Qiao Y, Wu D, Chen J G, Wang J, Guo F M and Yang Y J 2019 *Phys. Rev. A* **100** 063428
[13] Baykusheva D, Brennecke S, Lein M and Wörner H J 2017 *Phys. Rev. Lett.* **119** 203201
[14] Kfir O, Grychtol P, Turgut E, Knut R, Zusin D, Popmintchev D, Popmintchev T, Nembach H, Shaw J M, Fleischer A, Kapteyn H, Murnane M and Cohen O 2015 *Nat. Photon.* **9** 99
[15] Rajpoot R, Holkundkar A R and Bandyopadhyay J N 2021 *J. Phys. B: At. Mol. Opt. Phys.* **54** 225401
[16] Medišauskas L, Wragg J, van der Hart H and Ivanov M Y 2015 *Phys. Rev. Lett.* **115** 153001
[17] Jiménez-Galán Á, Zhavoronkov N, Ayuso D, Morales F, Patchkovskii S, Schloz M, Pisanty E, Smirnova O and Ivanov M 2018 *Phys. Rev. A* **97** 023409
[18] Dixit G, Jiménez-Galán Á, Medišauskas L and Ivanov M 2018 *Phys. Rev. A* **98** 053402
[19] Li M Z, Xu Y, Jia G R and Bian X B 2019 *Phys. Rev. A* **100** 033410
[20] Yuan K J and Bandrauk A D 2019 *Phys. Rev. A* **100** 033420
[21] Liu X, Zhu X, Li L, Li Y, Zhang Q, Lan P and Lu P 2016 *Phys. Rev. A* **94** 033410
[22] Wang D, Zhu X, Yuan H, Lan P and Lu P 2020 *Phys. Rev. A* **101** 023406
[23] Bandrauk A D, Mauger F and Yuan K J 2016 *J. Phys. B: At. Mol. Opt. Phys.* **49** 23LT01
[24] Mauger F, Bandrauk A D and Uzer T 2016 *J. Phys. B: At. Mol. Opt. Phys.* **49** 10LT01
[25] Yuan K J, Chelkowski S and Bandrauk A D 2021 *J. Phys. Chem. A* **125** 7111
[26] Neufeld O and Cohen O 2019 *Phys. Rev. Lett.* **123** 103202
[27] Zhou S, Li Q, Guo F, Wang J, Chen J and Yang Y 2021 *Chem. Phys.* **545** 111147
[28] Lei Z X, Yan S J, Hao X Y, Ma P, Zhou S P and Guo J 2023 *Commun. Theor. Phys.* **75** 065501
[29] Baykusheva D, Ahsan M S, Lin N and Wörner H J 2016 *Phys. Rev. Lett.* **116** 123001
[30] Feit M D, Fleck J A and Steiger A 1982 *J. Comput. Phys.* **47** 412
[31] Odžak S and Milošević D B 2015 *Phys. Rev. A* **92** 053416
[32] Zhang X, Li L, Zhu X, Liu X, Zhang Q, Lan P and Lu P 2016 *Phys. Rev. A* **94** 053408
[33] Barreau L, Veyrinas K, Gruson V, Weber S J, Auguste T, Hergott J F, Lepetit F, Carré B, Houver J C, Dowek D and Salières P 2018 *Nat. Commun.* **9** 4727
[34] Yuan K J and Bandrauk A D 2020 *Phys. Chem. Chem. Phys.* **22** 325
[35] Zhang B and Lein M 2019 *Phys. Rev. A* **100** 043401
[36] Milošević D B 2015 *Opt. Lett.* **40** 2381
[37] Bertrand J B, Wörner H J, Bandulet H C, Bisson É, Spanner M, Kieffer J C, Villeneuve D M and Corkum P B 2011 *Phys. Rev. Lett.* **106** 023001
[38] Zhang S Q, Zhang B, Jiang X Q and Sun X D 2023 *J. Phys. B: At. Mol. Opt. Phys.* **56** 105603